2023

Role of Endoplasmic Reticulum Stress Response in Parainfluenza Virus Acute to Persistent Infections

Lauren L. Abbitt
University of Central Florida

ROLE OF ENDOPLASMIC RETICULUM STRESS RESPONSE IN PARAINFLUENZA VIRUS ACUTE TO PERSISTENT INFECTIONS

by

LAUREN L. ABBITT

A thesis submitted in partial fulfillment of the requirements
for the Honors Undergraduate Thesis Program in Biomedical Sciences
in the College of Medicine
and in the Burnett Honors College
at the University of Central Florida
Orlando, Florida

Spring Term
2023

Thesis Chair: Griffith Parks, Ph.D.

Abstract

Persistent viral infections are a major health concern, with persistently infected (PI) cells being a source of continued shedding of virus and generation of viral mutants. Here, we hypothesized that cells persistently infected with the enveloped virus parainfluenza virus 5 (PIV5) would show altered expression of endoplasmic reticulum (ER) stress proteins and increased resistance to death caused by drug-induced ER stress. To test this, lysates of mock-infected, PIV5 acute-infected, and PIV5 PI human lung A549 cells were collected and levels of ER stress proteins were compared. Western blotting revealed that immunoglobulin heavy chain binding protein (BiP/GRP78) was present in higher levels in acute-infected and PI cells compared to naïve cells, indicating increased ER stress in both acutely infected and PI cells. Interestingly, basal levels of the ER stress-sensing protein IRE1α were upregulated in PI compared to naïve and acutely infected cells, but PI cells showed decreased activation of IRE1α compared to acutely infected cells. Naïve, acute-infected, and PI A549-NLR cells were treated with ER stress-inducing drugs tunicamycin, thapsigargin, and epigallocatechin gallate and monitored in real-time viability assays for drug-induced cell death. PI cells showed lower levels of stress-induced cell death compared to naive cells, whereas acute-infected cells experienced the greatest extent of cell death when challenged with ER stress-inducing drugs. Together, these results support the hypothesis that PIV5 persistently infected cells display altered ER stress response pathways and that PI cells are more resistant to death caused by ER stress-inducing drugs. Additionally, these results suggest that IRE1α plays a key role in the shift from acute to persistent infection. These results have implications for the treatment of persistent viral infections, as well as the potential for these viruses to be used for oncolytic virotherapy in the future.

Acknowledgements

I would like to extend my sincere thanks to Dr. Griffith Parks for the mentorship and guidance he has provided me throughout this experience. I would also like to thank my committee members Dr. Alicja Copik and Dr. Travis Jewett for their feedback throughout this process. Additionally, I am extremely grateful for the guidance the members of the Parks Lab have provided me, especially Dr. Candace Fox; this would not have been possible without them. Lastly, I would like to thank my family, my roommates, and my partner for the support and encouragement they have provided me throughout this process.

Table of Contents

List of Figures

Introduction

Oncolytic virotherapy is becoming an increasingly compelling treatment for cancer. Currently, talimogene laherparepvec (T-VEC) is the only oncolytic virus approved by the FDA for cancer treatment.[1] Ideal oncolytic viruses are able to infect and replicate in cancer cells to cause extensive cell death, without harming or replicating in normal cells.[2] Many viruses are being studied for oncolytic activity and therapeutic potential, and paramyxoviruses show great promise for oncolytic virotherapy due to their extensive cytopathic capabilities and ability to stimulate host immune response.[3]

Paramyxoviruses are characterized as being enveloped, negative-sense, single-stranded RNA viruses.[4] Viruses of the *paramyxoviridae* family are known to cause diseases such as measles, mumps, and croup; they can also cause both upper and lower respiratory tract infections.[5,6] An atypical member of the *paramyxoviridae* family is parainfluenza virus 5 (PIV5). This virus is an outlier because it is largely noncytopathic, whereas paramyxoviruses typically demonstrate great cytopathic ability.[7] The exact causes of wild-type (WT) PIV5's lack of cytopathicity are not well understood at this time.[8] WT PIV5 contains seven genes, with the shared P/V region being involved in cytopathic capabilities.[4] The V protein has been implicated in suppression of interferon (IFN) response, as it targets STAT1 for degradation.[9] Through the destruction of STAT1, WT PIV5 is capable of infecting cells without triggering an IFN response.

In this study, a PIV5 mutant with an alteration in the P/V region (P/V PIV5) was used. In P/V PIV5, the gene coding for the V protein has been mutated to be inactive, preventing P/V PIV5 from suppressing IFN response in the host cell.[8] This allows for IFN response activation in cells that are capable of normal IFN response. In these normal cells, the IFN response prevents P/V

PIV5 from proliferating and spreading. However, in cancer cells, IFN response pathways are suppressed.[2] Therefore, P/V PIV5 is able to proliferate in cancer cells, but not in normal cells. The alterations in the P/V region also confer P/V PIV5 with high cytotoxicity. The combined selectivity and cytopathicity of P/V PIV5 make it a promising candidate for oncolytic virotherapy.

A pitfall of using paramyxoviruses as oncolytic agents is that they are known to cause persistent infections in host cells.[6] For the purpose of this study, a persistent infection is defined as beginning as an acute infection, but infected cells do not clear the virus or die. Instead, infected cells continue to grow and shed virus. Because these persistently infected cells do not die, anti-tumor efficacy of paramyxovirus oncolytic agents is decreased. A previous study showed that P/V PIV5 is capable of establishing persistent infection in cancer cells.[8] This finding displayed an issue with using P/V PIV5 as an oncolytic virus: if cancer cells become persistently infected, they are not killed. Additionally, because the viral infection is not cleared in such cells, the host continues to harbor and shed the virus for however long the infection lasts. Although P/V PIV5 is susceptible to IFN response and would in theory be eliminated in noncancerous cells, continuous shedding of virus from PI cancer cells is not ideal.[5]

This finding that P/V PIV5 can establish persistent infection led to the following question: how can cells survive infection by a cytopathic virus without clearing this virus? It has been proposed that apoptotic pathways are altered in these cells that harbor P/V PIV5 for extended periods of time.[8] Enveloped viruses such as paramyxoviruses typically impose stress on host cells by increasing flux of viral glycoproteins through the secretory system, leading to activation of endoplasmic reticulum (ER) stress response pathways. ER stress occurs when ER machinery cannot maintain processing levels of proteins that the cell demands of it, resulting in accumulation of unfolded or misfolded proteins.[10] This buildup of defective proteins leads to the activation of

the unfolded protein response (UPR). The UPR initially increases the protein folding capacity of the cell, but if stress persists, it triggers apoptosis.[10,11 12] P/V PIV5 infection leads to increased ER stress due to the added load of glycosylating and folding viral membrane proteins HN (responsible for cell attachment) and F (responsible for cell fusion).[4,12] It is possible that P/V PIV5 acute-infected cells are overwhelmed by this stress, and PI cells are capable of overcoming it.

In this study, the possibility of P/V PIV5 infection altering host cell ER stress response pathways was tested as a potential contributor to the shift from acute to persistent P/V PIV5 infection. The results support our hypothesis that PI cells show altered expression of ER stress response proteins and that PI cells are be more resistant to drug-induced ER stress than naïve cells and cells acutely infected with P/V PIV5.

Materials and Methods

Cells and Virus

Human adenocarcinomic lung A549 cells expressing a nuclear protein that fluoresces red (A549-NLR cells) were purchased from Incucyte.[13] P/V PIV5 expressing green fluorescent protein (GFP) was utilized.[4] A549-NLR cells with previously established persistent P/V PIV5 infection were also utilized.

Infections for Lysate Collection

Naïve A549-NLR cells were cultured in two six-well plates and P/V PIV5 persistently infected A549-NLR cells were cultured in one 6-well plate. At 90% confluence, one plate of naïve A549-NLR cells was infected with P/V PIV5 to generate the acute infection group. A 1:20 dilution of the P/V PIV5 stock was produced using a 1:10 BSA/0% DMEM mixture, and each well of the acute infection group was treated with one mL of the 1:20 diluted P/V PIV5 stock such that MOI was approximately two pfu/cell in each well. The remaining plate of naïve A549-NLR cells was mock infected, with each well receiving 1 mL of 0% DMEM. The mock- and acute-infected cells then incubated at 37 degrees C for one hour to ensure infection synchronization.

After the incubation time, the media was removed from each well, and each well was washed with PBS+. Each well was treated with protein lysis buffer (PLB) for two minutes, then the wells were scraped and drained to harvest cells into one tube per cell group to produce a homogenous mixture of mock-infected cells and a separate homogenous mixture of acute-infected cells. Each mixture was then divided into 250 uL aliquots, boiled for five minutes, and

stored at -20 degrees C. This process was repeated for the six-well plate of persistently infected cells beginning after the incubation period.

Western Blotting

Lysates of mock-, acute- and persistent-infected cells were resolved on 10% sodium dodecyl sulfate-polyacrylamide gel electrophoresis (SDS-PAGE) gels, then transferred to nitrocellulose membranes using semi-dry transfer. The membranes were then treated with primary antibodies, followed by secondary antibodies conjugated to horseradish peroxidase (HRP). The following antibodies were used:

i. Mouse anti-actin (1:5000 dilution, Sigma-Aldrich, St. Louis, MO, USA)

ii. Rabbit anti-BiP (1:1000, Cell Signaling Technology, Danvers, MA, USA)

iii. Rabbit anti-PDI (1:1000, Cell Signaling Technology)

iv. Rabbit anti- IRE1α (1:1000, Cell Signaling Technology)

v. Rabbit anti-phosphorylated IRE1α (1:500, Novus Biologicals, Centennial, CO)

vi. Goat anti-mouse HRP (1:5000, Sigma-Aldrich)

vii. Anti-rabbit HRP (1:2000, Cell Signaling Technology)

Blots were visualized using the ChemiDoc Imaging System (Bio-Rad, Hercules, CA, USA), and samples were normalized to β-actin.

Infections for Cell Viability Assays

Naïve A549 cells and P/V PIV5 persistently infected cells expressing a red fluorescent protein (A549-NLR) were plated in 96-well plates (Corning, NY, USA) at 7,000 cells/well and left in the incubator at 37 °C. Once the cells reached at least 80% confluence, a portion of the naïve cells

were infected with P/V PIV5 to generate the acute infection group. 7 uL of 3.4X10^7 pfu/mL P/V PIV5 stock were added to each well of the acute infection group (MOI approximately 23 pfu/cell). The cells then incubated at 37 °C for one hour to ensure infection synchronization, after which each well was drained of media, washed with PBS+, and received 50 uL of 2% DMEM. The cells were then incubated at 37 °C for six hours. After this six-hour incubation, cells were treated with ER stress-inducing drugs.

Drug Treatments

The naïve, acute-infected, and PI cells were treated with the following drugs six hours post infection:

i. Tunicamycin (Fisher Scientific)

ii. Thapsigargin (Sigma-Aldrich)

iii. Epigallocatechin gallate (Sigma-Aldrich)

Drug stocks were generously prepared by the Parks lab using deionized, sterile water for EGCG and dimethyl sulfoxide (DMSO) for tunicamycin and thapsigargin. Drug dilutions were prepared using these stocks and 2% DMEM during the six-hour period between infection and drug treatment. These dilutions were prepared such that 50 uL of drug-medium mixture would be added to each well, resulting in a total of 100 uL liquid per well (50 uL drug-medium mixture with 50 uL medium already present in each well). Replacing of media was intentionally limited to minimize additional stress imposed on the cells.

At the time of treatment, three wells of each infection condition (naïve, acute-infected, and PI) were treated with the same drug concentration. Multiple concentrations were tested for each drug, and three wells of each infection condition were dedicated to an untreated control of

2% DMEM, in addition to three wells of each infection condition being dedicated to DMSO control.

Cell Viability Assay

Immediately after drug treatment, cells were placed in the Incucyte S3 Live-Cell Analysis system (Sartorius) at 37 °C for two to three days. Images were captured every two hours using 10x objective in red and phase channels. Red Object Count (ROC) was measured at each time images were captured.

Statistical Analyses

GraphPad Prism was used to normalize ROC to the ROC at time zero (ROC/ROC^{t0}) and to calculate the average ROC/ROC^{t0} between wells of the same infection and drug treatment conditions. Graphs were generated to display ROC normalized to ROC at time zero over time, with standard error calculated and shown at each data point.

Results

Persistently Infected Cells Display Differential Expression and Activation of IRE1α

To determine if the expression of ER stress proteins was altered in PI cells compared to naïve and acutely infected cells, relative expression levels of the following proteins were compared using western blotting:

i. Immunoglobulin heavy chain binding protein (**BiP**), a protein found in the eukaryotic ER that facilitates correct folding of other proteins produced in the cell.[14] BiP is also known as Glucose-Regulated Protein 78 (GRP78). When a cell experiences ER stress, expression of BiP is expected to increase.

ii. Protein disulfide isomerase (**PDI**), an enzyme that assists with disulfide bond formation within or between proteins of the ER.[11] When a cell experiences ER stress, PDI expression is expected to increase.

iii. Inositol-requiring gene 1 (**IRE1α**), a transmembrane protein of the ER that can trigger the UPR. Under acute ER stress, activation of IRE1α leads to increased folding capacity of the cell. Activation of IRE1α under prolonged ER stress can lead to apoptosis.[11] Phosphorylation of IRE1α indicates that it has been activated.[15]

Lysates of mock-infected, P/V PIV5 acutely infected, and P/V PIV5 persistently infected cells were collected and analyzed using western blotting. Band intensity was compared between samples to determine relative protein expression, with more intense bands indicating greater expression.

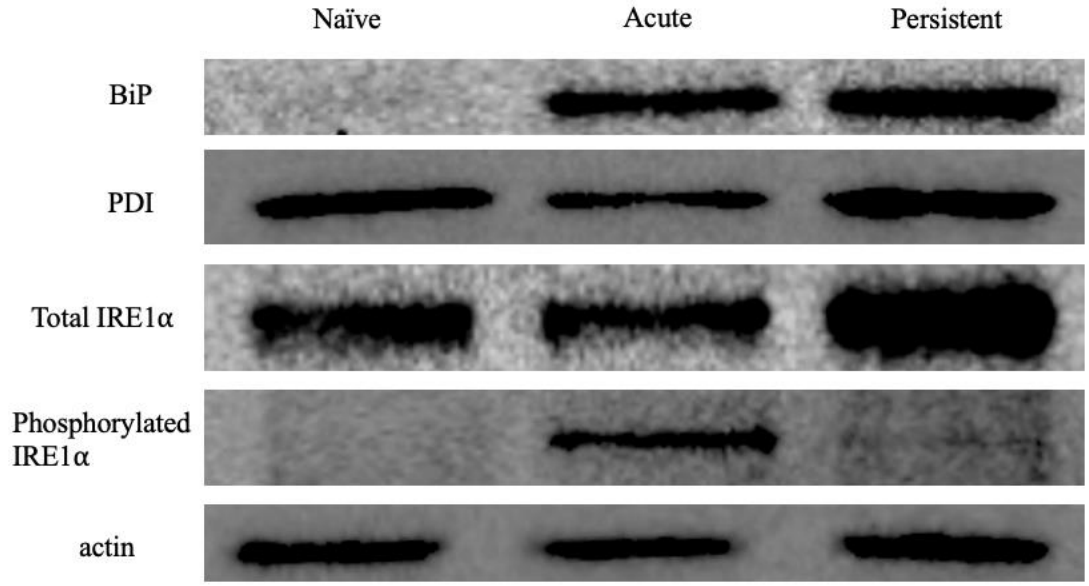

Figure 1: Western blotting revealed differential IRE1α expression and activation in PI cells compared to acutely infected and naïve cells.

Lysates were collected from naïve, PIV5 P/V acute-infected, and PIV5 P/V PI cells, then probed for BiP, PDI, total IRE1α, and phosphorylated IRE1α. Samples were normalized to β-actin.

As shown in Figure 1, there was no substantial difference in BiP expression between acutely and persistently infected cells; however, both acute-infected and PI cells expressed BiP, whereas naïve cells did not show a clear signal when probed for BiP. There was no prominent difference in PDI expression between conditions. The band intensity for total IRE1α was greatest in the PI cell lysate compared to the naïve and acute-infected cell lysates, but there was no major difference between band intensities of the naïve and acute-infected cell lysates. The most striking difference was seen when the lysates were probed for phosphorylated IRE1α. A clear band for phosphorylated/activated IRE1α was only present in the acute-infected cell lysate. Together, these data support the hypothesis that the ER stress response is altered in the shift from acute to persistent infection.

Persistently Infected Cells Show Increased Resistance to Death Mediated by ER Stress-Inducing Drugs

The following drugs were used to induce ER stress:

i. **Tunicamycin**, which induces ER stress by inhibiting glycosylation of proteins in the ER. This results in accumulation of defective proteins and ER stress.[16]

ii. **Thapsigargin**, which causes Ca^{2+} imbalance and thus stress in the ER by inhibiting the Ca^{2+}-ATPase pump.[17] This Ca^{2+} imbalance activates the UPR and eventually triggers apoptosis via CHOP.[11,18]

iii. **Epigallocatechin gallate** (EGCG), which has been shown to cause ER stress in cancer cells by increasing expression of BiP and ER stress sensor PERK (protein kinase RNA like ER kinase), by increasing expression and activation of IRE1α, and by upregulating and activating eIF2 and ATF4 (downstream effectors of PERK) in addition to XBP1 (downstream effector of IRE1α) and CHOP.[19,20]

Tunicamycin

To determine the kinetics of cell killing by tunicamycin, A549 cells that stably express a red fluorescent protein in the nucleus (A549-NLR) were used. Loss of red fluorescence in A549-NLR cells indicates loss of intact nuclei, so these cells can be monitored by the fluorescence detector in the IncuCyte instrument to gain a readout for number of cells with intact nuclei over time. At each timepoint, the data were expressed as remaining Red Object Count (ROC) normalized to the ROC recorded at time zero, immediately after drug treatment (ROC/ROC^{t0}). ROC/ROC^{t0} is expressed as a percentage. A549-NLR naïve, acute-infected, or PI cells were treated with 35 ug/mL tunicamycin and scanned every two hours post drug treatment to monitor red fluorescence, which is expressed here as ROC/ROC^{t0}.

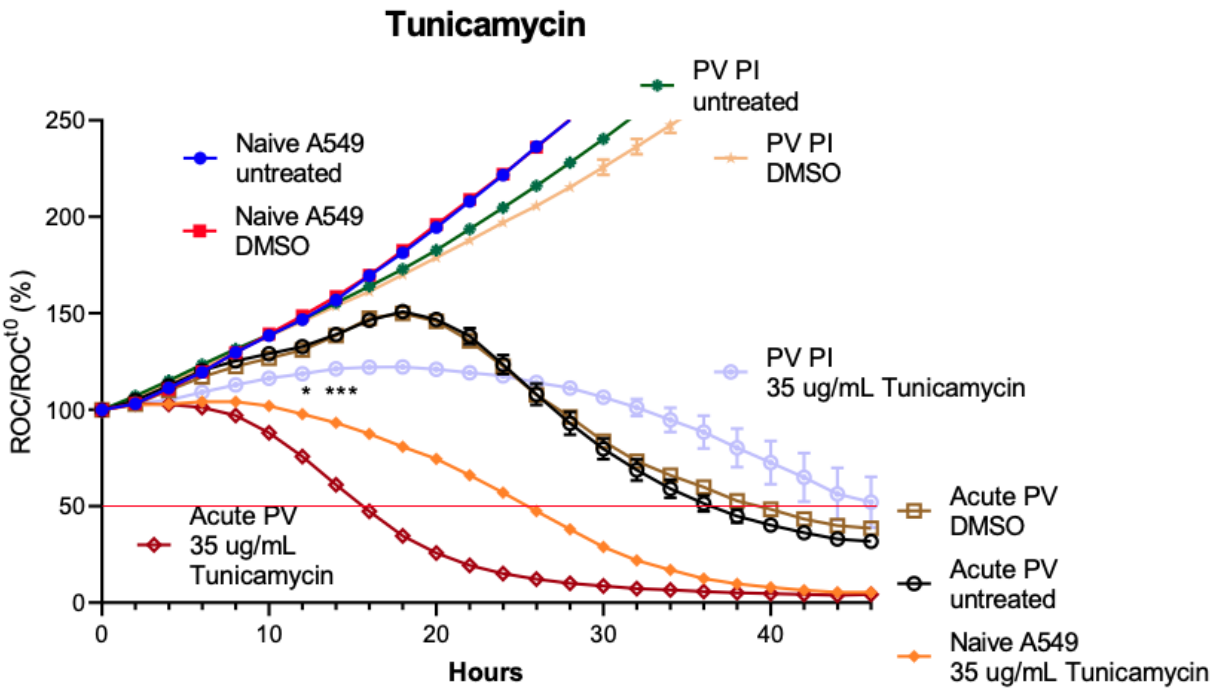

Figure 2: Lung cells persistently infected with P/V PIV5 and treated with 35 ug/mL tunicamycin showed lesser decrease in red fluorescence than did naïve and acutely infected cells over time.

*A549-NLR cells expressing nuclear red fluorescent protein were mock infected, acutely, or persistently infected with P/V PIV5. Each cell group was left untreated in 2% DMEM, DMSO, or treated with tunicamycin at a concentration of 35 ug/mL. The IncuCyte instrument was used to capture images of the cells and measure red object count (ROC) per well at two hour intervals over 46 hours. ROC was normalized to reflect the percent of red objects present at time zero, directly after drug treatment (ROC/ROC^{t0}). Each value in the figure represents the average of three replicates, with bars reflecting standard error. * indicates a P-value of < 0.05, ** indicates a P-value of < 0.01, and *** indicates a P-value of < 0.001 comparing PI cells to naïve cells. The red horizontal line indicates 50% ROC/ROC^{t0}.*

As shown in Figure 2, untreated and DMSO-only naïve and PI cells continue to proliferate over the time they were monitored, with ROC/ROC^{t0} never falling below 100%. Untreated DMSO-only acute-infected cells (brown and black curves) initially proliferated, exhibiting a peak ROC/ROC^{t0} of 149.95% at 18 hours. After this timepoint, these cells began to exhibit more extensive death than growth, with ROC/ROC^{t0} decreasing for the remaining time monitored and falling to 38.60% at 46 hours.

Naïve A549 cells treated with 35 ug/mL tunicamycin (orange curve) showed slight initial proliferation, peaking at 104.17% ROC/ROC^{t0} at 8 hours post treatment, then decreasing after this time. These cells' ROC/ROC^{t0} fell below 10% at 38 hours post treatment, and fell to a minimum of 5.34% ROC/ROC^{t0} at 46 hours post treatment. Acute-infected cells treated with 35 ug/mL tunicamycin (burgundy curve) showed the most extensive cell death, with ROC/ROC^{t0} peaking at 103.27% ROC/ROC^{t0} at only 2 hours post treatment, then exhibiting a steady decrease until 44 hours post treatment. These cells' ROC/ROC^{t0} remained within 4-6% ROC/ROC^{t0} for the rest of time monitored beginning at 36 hours post treatment.

PI cells treated with 35 ug/mL tunicamycin (light purple curve) initially showed proliferation, although it was less pronounced than the other groups of cells that exhibited early proliferation. At 18 hours post treatment, these tunicamycin-treated PI cells' ROC/ROC^{t0} peaked at 122.27%, then began to decrease, showing that cell death was greater than proliferation after this point. Although tunicamycin-treated PI cells' viability declined after 18 hours post treatment, their ROC/ROC^{t0} did not fall below 50% over the entire time they were monitored. This finding may be compared to the findings that acute-infected cells' and tunicamycin-treated naïve cells' ROC/ROC^{t0} fell below 50% at 16 hours and 26 hours, respectively.

When treated with 35 ug/mL tunicamycin, a significant difference in ROC/ROC^{t0} between PI and naïve cells beginning at 12 hours post drug treatment was observed (P-value < 0.05). This difference became more significant at 14 hours (P-value < 0.001). Because acute-infected cells treated with 35 ug/mL tunicamycin displayed decreased ROC/ROC^{t0} compared to naïve cells during this time, the difference between PI and acute-infected cells was also significant.

In summary, the curves of most interest are those showing the viability of tunicamycin-treated cells: PI (light purple curve), acute-infected (burgundy curve), and naïve (orange curve) cells. These curves reflect increased viability of PI cells compared to both naïve and acute-infected cells when treated with 35 ug/mL tunicamycin. Together, these data support the hypothesis that PI cells are more resistant to death mediated by ER stress-inducing drugs than naïve and acute-infected cells.

Thapsigargin

To determine the kinetics of cell killing by thapsigargin, A549-NLR naïve, acute-infected, and PI cells were treated with 10 uM thapsigargin and monitored using the same method described for tunicamycin treatment. ROC/ROC^{t0} was recorded for each cell group at each timepoint, at two-hour increments.

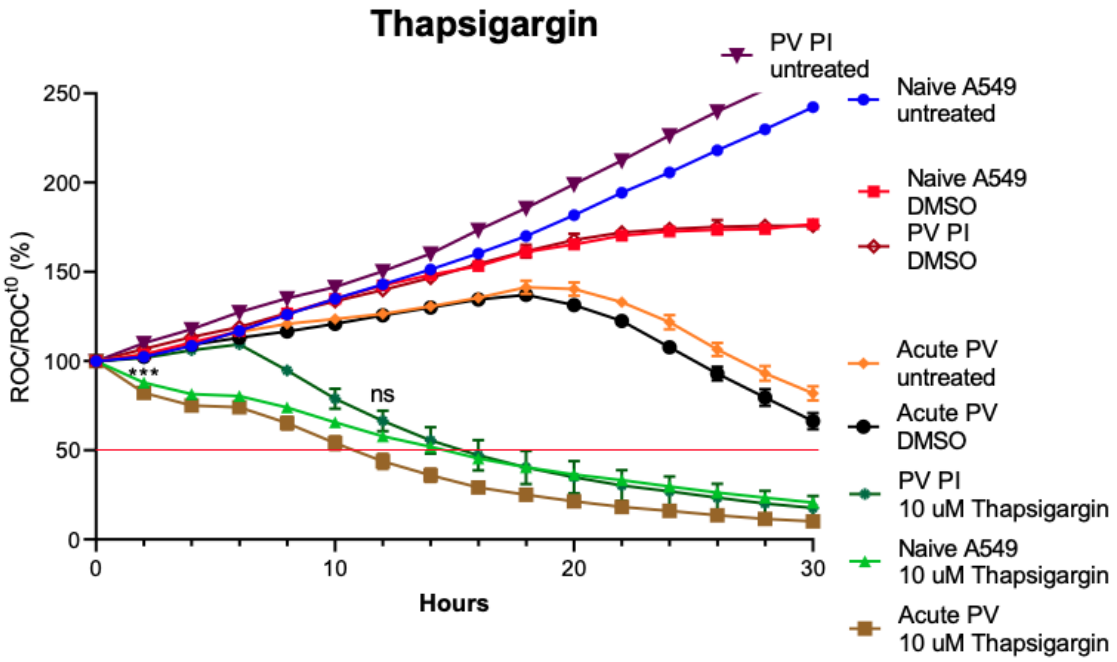

Figure 3: Lung cells persistently infected with P/V PIV5 and treated with 10 uM thapsigargin showed lesser decrease in red fluorescence than did naïve and acutely infected cells over a short period of time.

*A549-NLR cells expressing nuclear red fluorescent protein were mock infected, acutely, or persistently infected with P/V PIV5. Each cell group was left untreated in 2% DMEM, DMSO, or treated with thapsigargin at a concentration of 10 uM. The IncuCyte instrument was used to capture images of the cells and measure red object count (ROC) per well at two hour intervals over 68 hours. ROC was normalized to reflect the percent of red objects present at time zero, immediately after drug treatment (ROC/ROC^{t0}). Each value in the figure represents the average of three replicates, with bars reflecting standard error. * indicates a P-value of < 0.05, ** indicates a P-value of < 0.01, and *** indicates a P-value of < 0.001 comparing PI cells to naïve cells. Loss of significance is indicated by "ns" and 50% ROC/ROC^{t0} is represented by a red horizontal line.*

As shown in Figure 3, untreated and DMSO-only PI (burgundy curve) and naïve cells (red curve) exhibited proliferation over the time they were monitored, without any major decreases in ROC/ROC^{t0}. This proliferation is represented by ROC/ROC^{t0} rising above 100% and continuing to increase over time. DMSO-only naïve and PI cells' ROC/ROC^{t0} increased less rapidly beginning at 22 hours post treatment, remaining between 172% and 176% until 30 hours post treatment. After this time, DMSO-only naïve cells remained between 178% and 184% ROC/ROC^{t0} for the remainder of time monitored, increasing and decreasing until monitoring was

ceased (not shown). After 30 hours post treatment, DMSO-only PI cells' ROC/ROC^{t0} decreased gradually from 174.56% to 122.93% over the remainder of time monitored (not shown).

Untreated and DMSO-only acute-infected cells (orange and black curves) both showed initial proliferation, with untreated acute-infected cells peaking at 141.32% and DMSO-only acute-infected cells peaking at 137.03% ROC/ROC^{t0} at 18 hours post treatment. After this time, both groups' ROC/ROC^{t0} decreased for the remainder of time monitored, indicating greater cell death than growth.

Naïve A549-NLR cells treated with 10 uM thapsigargin (light green curve) did not display pronounced proliferation at any time. Instead, ROC/ROC^{t0} steadily decreased over time, falling below 50% and 10% ROC/ROC^{t0} at 16 and 46 hours, respectively. At the last timepoint monitored (68 hours post treatment), these cells reached their minimum ROC/ROC^{t0} of 3.80% (not shown). Acute-infected cells treated with 10 uM thapsigargin (brown curve) did not proliferate during the time monitored, but showed a steady decrease in ROC/ROC^{t0} for the entirety of time monitored. These cells fell below 50% ROC/ROC^{t0} at 12 hours post treatment, 10% ROC/ROC^{t0} at 32 hours post treatment, and 5% ROC/ROC^{t0} at 42 hours post treatment (not shown).

PI cells treated with 10 uM thapsigargin (dark green curve) showed slight proliferation initially with ROC/ROC^{t0} peaking at 109.41% at 6 hours post treatment, but ROC/ROC^{t0} decreased steadily after this time, falling below 50% and 10% ROC/ROC^{t0} at 16 and 40 hours, respectively.

When treated with 10 uM thapsigargin, a significant difference in ROC/ROC^{t0} between PI and naïve cells beginning at two hours post drug treatment was observed (P-value < 0.001). This difference became insignificant at 12 hours post treatment. A significant difference in

ROC/ROC^{t0} between PI and acute-infected cells began at 2 hours post drug treatment (P-value < .0001, with PI cells being more viable than acute-infected cells. Significance decreased at 18 hours post treatment (P-value < .001), 20 hours post treatment (P-value < .01), and 22 hours post treatment (P-value < .05), with the difference in ROC/ROC^{t0} between PI and acute-infected cells becoming insignificant at 24 hours post treatment.

In summary, the curves of greatest interest are those of thapsigargin-treated cells: PI (dark green curve), acute-infected (brown curve), and naïve (light green curve). These curves show the temporarily increased viability of PI cells compared to both naïve and acute-infected cells when treated with 10 uM thapsigargin, and that PI cells are not significantly more viable than naïve cells after 12 hours post treatment. Although not shown on the graph, the difference in cell viability between PI and acute-infected cells treated with 10 uM thapsigargin becomes insignificant after 24 hours post treatment. Together, these data support the hypothesis that PI cells are more resistant to death mediated by ER stress-inducing drugs than naïve and acutely infected cells. However, this resistance appeared to be present only in the initial hours after drug treatment, with PI cell viability becoming more similar to that of naïve and acute-infected cells as time passed.

Epigallocatechin Gallate (EGCG)

To determine the kinetics of cell killing, A549-NLR naïve, acute-infected, and PI cells were treated with 50 uM EGCG and monitored using the same method described for tunicamycin treatment. ROC/ROC^{t0} was recorded for each cell group at each timepoint, at two-hour increments.

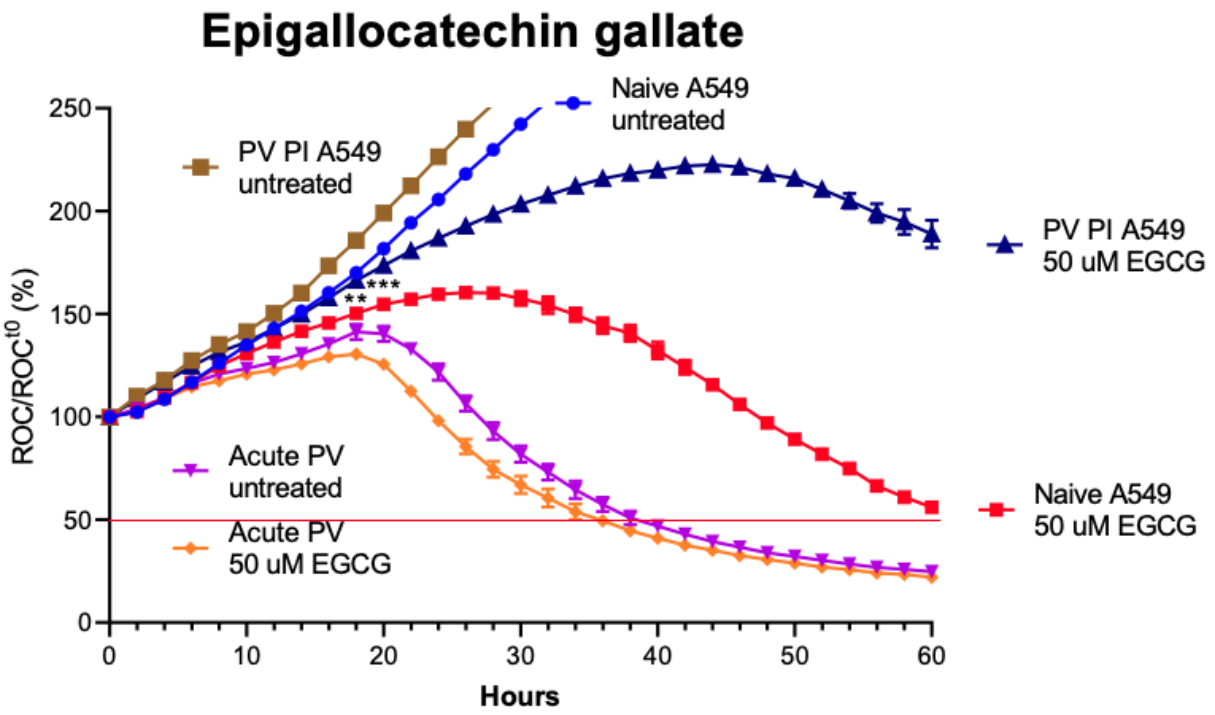

Figure 4: Lung cells persistently infected with P/V PIV5 and treated with 50 uM EGCG showed lesser decrease in red fluorescence than did naïve and acutely infected cells over time.

*A549-NLR cells expressing nuclear red fluorescent protein were mock infected, acutely, or persistently infected with P/V PIV5. Each cell group was left untreated in 2% DMEM or treated with EGCG at a concentration of 50 uM. The IncuCyte instrument was used to capture images of the cells and measure red object count (ROC) per well at two-hour intervals over 68 hours. ROC was normalized to reflect the percent of red objects present at time zero (immediately after drug treatment), represented by ROC/ROC^{t0}. Each value in the figure represents the average of three replicates, with bars reflecting standard error. * indicates a P-value of < 0.05, ** indicates a P-value of < 0.01, and *** indicates a P-value of < 0.001 comparing PI cells to naïve cells. The red horizontal line represents 50% ROC/ROC^{t0}*

.

As Figure 4 displays, untreated naïve and PI cells (brown and royal blue curves) showed extensive proliferation, exceeding 250% ROC/ROC^{t0} after 26 hours and 24 hours, respectively. Untreated acute-infected A549-NLR cells (purple curve) initially proliferated, with ROC/ROC^{t0} peaking at 141.32% at 18 hours post treatment. After this point, ROC/ROC^{t0} for these cells decreased steadily for the remainder of time monitored, falling below 50% between 38 and 40 hours and falling to a minimum of 20.22% at the end of time monitored (68 hours total).

Naïve cells treated with 50 uM EGCG (red curve) initially proliferated, with ROC/ROC^{t0} increasing to a peak of 160.44% at 26 hours post treatment. After this time, these cells experienced a steady decrease in ROC/ROC^{t0} until monitoring was complete at 68 hours post treatment, ending with an ROC/ROC^{t0} of 40.29%. Acutely infected cells treated with 50 uM EGCG (orange curve) initially proliferated, displayed by ROC/ROC^{t0} increase until 18 hours post treatment, with a peak of 130.47%. After this point, these cells experienced a steady decrease in ROC/ROC^{t0} for the remainder of the time they were monitored, falling to 18.99% at the last scan time (total of 68 hours).

PI cells treated with 50 uM EGCG (navy blue curve) displayed proliferation for the majority of the time they were monitored, reaching their peak ROC/ROC^{t0} of 222.68% at 44 hours post treatment. After this point, ROC/ROC^{t0} decreased until monitoring was stopped at 68 hours post treatment, with ROC/ROC^{t0} falling to 166.70% (not shown).

When treated with 50 uM EGCG, a significant difference in ROC/ROC^{t0} between PI and naïve cells beginning at 18 hours post drug treatment was observed (P-value < 0.01), with PI cells being more resistant to death. This difference became more significant at 20 hours (P-value < 0.001) and remained for the rest of the time the cells were monitored. Because acute-infected cells treated with 50 uM EGCG displayed decreased ROC/ROC^{t0} compared to naïve cells, the difference between PI and acute-infected cells was also significant. Out of the cells treated with 50 uM EGCG, only the PI cells' ROC/ROC^{t0} did not fall below 50%.

In summary, the curves of greatest importance are those showing the viability of EGCG-treated cells: PI (navy blue curve), acute-infected (orange curve), and naïve (red curve). These curves reflect increased viability of PI cells compared to both naïve and acute-infected cells when treated with 50 uM EGCG. Together, these data support the hypothesis that PI cells are

more resistant to death caused by ER stress-inducing drugs than are naïve and acute-infected cells.

Discussion

Although P/V PIV5 shows great potential to be used as an oncolytic virus due to its cytopathic capabilities and selection for cancer cells, the ability of paramyxoviruses to establish a persistent infection is not ideal or well understood.[6,8]

ER Stress Response Protein Expression

In the first arm of this study, it was determined that persistent P/V PIV5 infection is associated with altered expression and activation of ER stress proteins, thus with alteration of ER stress response pathways.

BiP/GRP78

BiP was expressed in both acute-infected and PI cells but was present in much lower amounts in naïve cells, if present at all. BiP is upregulated when the cell is under ER stress to provide extra assistance to increase the cell's protein folding capacity.[14] Because the naïve cells were not challenged with ER stress by viral infection, they were expected to have lower levels of BiP compared to virus-infected cells. Because the band intensity for BiP was similar for the acute-infected and PI cells, both groups appeared to be experiencing ER stress and PI cells did not greatly suppress or increase BiP expression compared to acutely infected cells.

PDI

There was no major difference in band intensity of PDI between acute-infected, naïve, and PI cells, showing that PDI was present at similar levels between the groups. This indicates that a change in PDI expression is not solely responsible for the shift from acute to persistent P/V

PIV5 infection. This may also indicate that the viral proteins being expressed do not require additional PDI to be processed.

Total IRE1α

When probed for total IRE1α (both activated and inactivated), band intensity was similar between naïve and acute-infected cells. Interestingly, PI cell lysate showed the greatest band intensity compared to naïve and acute-infected cell lysates. This finding falls in line with expectations for the naïve cells; because they do not experience extensive ER stress, they have moderate basal levels of IRE1α. The acute-infected cells' total IRE1α band of similar intensity to the naïve cells showed that their levels of total IRE1α were close to basal levels present without viral infection. Because the PI cells had such a strong band when probed for total IRE1α, it was shown that total IRE1α levels were greatly increased compared to naïve and acute-infected cells, possibly due to the PI cells' prolonged infection leading to increased ER stress.

Phosphorylated IRE1α

Activation/phosphorylation of IRE1α indicates that the cell is experiencing ER stress, and that the UPR has been activated.[11,15] When considering that phosphorylated/activated IRE1α levels tend to increase due to increased ER stress, it may be expected that naïve cells show the lowest level of phosphorylated IRE1α, acute-infected cells show a higher level of phosphorylated IRE1α levels due to viral infection, and PI cells show the highest level of phosphorylated IRE1α expression due increased ER stress caused by prolonged viral infection. Additionally, because PI cells showed the highest level of total IRE1α compared to naïve and

acute-infected cells, PI cells may be expected to display the highest levels of phosphorylated IRE1α.

Unexpectedly, PI cells were shown to have a very low level of activated IRE1α compared to acute-infected cells. PI cells were shown to have a similar level of activated IRE1α compared to naïve cells. Despite PI cells' increased total IRE1α levels, they had lower activated IRE1α levels than acute-infected cells. These findings suggest that PI cells may be capable of inhibiting the phosphorylation/activation of IRE1α, potentially suppressing the pro-apoptotic UPR.

IRE1α is activated when BiP dissociates from it, causing IRE1α to dimerize and transphosphorylate.[21] Although preliminary, a potential explanation for PI cells' decreased IRE1α activation is that PI cells somehow prevent dimerization of IRE1α, thus preventing its activation via transphosphorylation. This may occur if PI cells are able to keep BiP from dissociating from IRE1α in response to ER stress; if BiP remains bound to IRE1α, then IRE1α cannot dimerize and activate. This may be determined in future experiments by characterizing BiP-IRE1α binding in PI cells compared to acute-infected and naïve cells using an affinity column and immunoblotting.

Drug-Treated Cell Viability

Because all cells treated with drugs tunicamycin, thapsigargin, and EGCG experienced enhanced ER stress compared to untreated cells, treated cells were expected to experience greater death than untreated cells. In addition to drug treatment, virus-infected cells also experienced heightened ER stress because viral infections demand greater protein production (and

glycosylation) from the host cell. The effects of persistent P/V PIV5 infection on ER stress are still being characterized; however, the acute-infected cells were expected to experience enhanced ER stress and death due to their dual stresses of drug treatment and viral infection. PI cells were hypothesized to experience increased resistance to death caused by ER stress-inducing drugs compared to both naïve and acute-infected cells.

In each group of cells challenged with ER stress-inducing drugs, PI cells were shown to have a trend of increased viability compared to naïve cells, and acute-infected cells showed the greatest decrease in viability over time compared to both naïve and PI cells.

Tunicamycin

When treated with 35 ug/mL tunicamycin, PI cells were shown to be more resistant to death than naïve and acute-infected cells. Tunicamycin causes ER stress by inhibiting N-linked glycosylation of proteins; it achieves this by preventing UDP-N-acetylglucoseamine (GlcNAc) from transferring to dolichol phosphate.[16] This prevents proper folding of glycosylated proteins, leading to the aggregation of misfolded proteins in the ER. Due to this aggregation of misfolded proteins, ER stress sensors and the UPR should be activated and induce apoptosis in cells with normal ER stress response pathways. Although preliminary, PI cells' resistance to tunicamycin-induced death may be explained by ER stress pathways being altered in persistently infected cells. In this case, misfolded proteins would still accumulate in the ER, but the UPR would not induce apoptosis as it normally would. This study's finding that ER stress sensor IRE1α's expression and activation is altered in PI cells support this notion, and future experiments may focus on determining if other parts of the ER stress response pathway are altered in PI cells. This may be achieved by determining relative expression of other ER stress proteins such as PERK using western blotting.

Alternatively, it is possible that cells persistently infected with P/V PIV5 express less viral proteins than acutely infected cells. In this case, the ER must glycosylate and properly fold a lower amount of viral glycoproteins HN and F, decreasing stress on the ER. This proposal may be tested by collecting lysates of naïve, P/V PIV5 acute-infected, and P/V PIV5 PI cells, then probing for viral proteins HN and F using western blotting. It is also possible that the same load of viral proteins is being sent through the ER in PI compared to acute-infected cells, but that a mutation in the viral genome has made viral proteins less dependent on glycosylation for proper folding. To determine if such mutation is present, the genome of P/V PIV5 that has been shown to establish persistent infection may be sequenced and compared to P/V PIV5 that has not been shown to establish persistent infection.

Thapsigargin

When treated with 10 uM thapsigargin, PI cells appeared to be more resistant to death than naïve and acute-infected cells for a short period after drug treatment. As with tunicamycin, these findings support the hypothesis that PI cells treated with thapsigargin were more resistant to death than naïve and acutely infected cells. However, this increased resistance of thapsigargin-treated PI cells to death did not persist, as PI cells showed similar viability to thapsigargin-treated naïve and acute-infected cells as time passed. Thapsigargin acts by inhibiting the sarco/endoplasmic reticulum calcium-ATPase (SERCA) pump in the ER, which is responsible for pumping calcium from the cytosol into the ER to maintain calcium homeostasis.[22] When the SERCA pump does not function as it is supposed to, calcium concentration increases in the cytosol and decreases in the ER lumen. Decreased calcium concentration in the endoplasmic reticulum causes ER stress, leading to apoptosis. It has been shown that death receptor 5 (DR5)

and caspase-8 are necessary for thapsigargin-induced apoptosis via ER stress; however, the exact mechanism of this is not understood.[18] Although preliminary, it is possible that PI cells alter the expression or function of DR5 and/or caspase-8 to increase resistance to thapsigargin-induced apoptosis compared to naïve and acute-infected cells. Although not completely understood, it is thought that the ER stress sensor PERK plays a role in upregulating and activating DR5 and caspase-8 through transcription factors ATF4 and CHOP.[23] Because of this, it may be feasible that PI cells gain resistance to ER stress-inducing drugs by impairing activation of PERK, or by altering its downstream effectors, although this notion is preliminary. Future experiments should aim to determine the activation and expression of PERK and its downstream effectors. This may involve probing for and comparing expression of PERK, CHOP, DR5 and caspase-8 in naïve, acute-infected, and PI cells lysates using western blotting.

Although PI cells treated with thapsigargin displayed resistance to death compared to naïve and acute-infected cells, this difference in viability was not sustained. This implies that PI cells are not as equipped to adapt to calcium imbalance compared to inhibition of N-glycosylation and ER stress sensor activation. This leads to the following question: why is this resistance only temporary? Although preliminary, it is possible that the pathway that PI cells use to confer initial resistance to thapsigargin-mediated death is overwhelmed, leading to death after a short period of resistance. In contrast, PI cells may be killed by an alternate mechanism. As previously discussed, thapsigargin acts by preventing the SERCA pump from moving calcium from the cytosol into the ER lumen, resulting in increased calcium concentration in the cytosol and decreased calcium concentration in the ER lumen.[22] It is possible that PI cells are resistant to death induced by calcium imbalance in the ER, but not resistant to death induced by calcium imbalance in the cytosol. Because cytosolic calcium plays roles in various cellular processes

including gene transcription, cell proliferation, exocytosis, and cell survival, it is possible that death is induced by a non-ER stress response pathway that PI cells are not prepared to adapt to. The activation of other apoptotic pathways may explain why thapsigargin-treated PI cells did not display the sustained difference in resistance to death that cells treated with tunicamycin and EGCG did. Before non-ER stress response pathways to apoptosis are explored, potential alterations of ER stress response pathways in PI cells treated with thapsigargin should first be characterized.

EGCG

When treated with 50 uM EGCG, PI cells showed increased resistance to killing compared to naïve and acute-infected cells. Thus, our hypothesis that PI cells would be more resistant to death mediated by ER stress-inducing drugs compared to naïve and acute-infected cells was supported. These results suggest that PI cells are equipped to circumvent killing resulting from EGCG-mediated ER stress. Although EGCG's effects on the ER stress response are not well characterized in A549 cells specifically, EGCG treatment has been shown to activate ER stress response pathways in other cancer cells primarily through increased BiP expression and upregulation/activation of IRE1α and PERK sensors and their downstream pathways.[19,20] Considering this, the following proposals for why PI cells are resistant to EGCG-mediated death are preliminary. EGCG-treated colorectal cancer cells have been shown to upregulate BiP, PERK, ATF4, IRE1α, and phosphorylation of eIF2α.[19] It is possible that EGCG causes these effects in cells with normal ER stress response pathways, but that PI cells are capable of preventing the upregulation of these effectors. This may be possible by preventing the activation of ER stress sensors IRE1α and PERK. Both sensors are activated in similar fashion: when BiP

dissociates from the sensor, the sensor dimerizes and autophosphorylates, activating its respective signaling cascade.[10,21] PI cells may prevent sensor autophosphorylation by inhibiting sensor dimerization; this could occur if BiP is kept from dissociating or if another molecule binds the sensor to hold the subunits apart. Future experiments should first focus on characterizing the effects of EGCG on ER stress response pathways in A549 cells. This may be achieved by treating uninfected A549 cells with EGCG, collecting lysates of these cells, then comparing ER stress protein expression and activation between treated and untreated cells using western blotting. This method can be repeated with EGCG-treated naïve, P/V PIV5 acute-infected, and PI cells to determine how ER stress protein expression is altered between EGCG-treated PI and acute-infected cells. BiP levels should be compared between samples to determine if it is being upregulated due to EGCG treatment. Additionally, binding between BiP and IRE1α or PERK can be characterized by using an affinity column to select for IRE1α or PERK, then probing the load for BiP.

Limitations

The findings that cells persistently infected with P/V PIV5 exhibit altered ER stress response pathways and are more resistant to death induced by ER stress-causing drugs suggest that the ER plays a major role in the shift from acute to persistent P/V PIV5 infection. However, it should be noted that this study only used human lung adenocarcinomic A549 cells. Other cancer cell types may react differently to persistent P/V PIV5 infection, so future studies should focus on characterizing persistent infection across cell types. This includes noncancerous cells, as it is unknown whether these cells respond to persistent viral infection similarly to cancerous cells. Additionally, this study only utilized P/V PIV5, a recombinant enveloped RNA virus.[4]

Cells persistently infected with P/V PIV5 may behave differently compared to cells persistently infected with a different virus; thus, other studies may focus on determining whether ER stress response pathways are implicated in the shift from acute to persistent infection by viruses other than P/V PIV5. This study was also limited in that ER stress protein levels were compared only between infection conditions; lysates were not collected from drug-treated cells. Because of this, effects of drug treatment on ER stress protein expression could not be characterized.

Future Directions

Future studies may focus on comparing drug-specific effects on ER stress protein expression between infection groups to determine which proteins are specifically involved in conferring PI cells resistance to death caused by these drugs. By determining how P/V PIV5 is capable of establishing persistent infections, other persistent viral infections may be better understood and treatments may be improved. Additionally, this would allow for better troubleshooting in the potential of using P/V PIV5 as an oncolytic virus. If the cause of the shift from acute to persistent P/V PIV5 infection can be understood, then future research may focus on preventing this shift to enhance tumor cell killing and decrease the risk of continued viral shedding.

References

1. Chaurasiya S, Fong Y, Warner SG. Oncolytic virotherapy for cancer: Clinical experience. *Biomedicines.* 2021;9(4). doi: 10.3390/biomedicines9040419.

2. Fukuhara H, Ino Y, Todo T. Oncolytic virus therapy: A new era of cancer treatment at dawn. *Cancer Sci.* 2016;107(10):1373-1379. doi: 10.1111/cas.13027.

3. Matveeva OV, Guo ZS, Shabalina SA, Chumakov PM. Oncolysis by paramyxoviruses: Multiple mechanisms contribute to therapeutic efficiency. *Mol Ther Oncolytics.* 2015;2:15011-. doi: 10.1038/mto.2015.11.

4. Wansley EK, Parks GD. Naturally occurring substitutions in the p/v gene convert the noncytopathic paramyxovirus simian virus 5 into a virus that induces alpha/beta interferon synthesis and cell death. *J Virol.* 2002;76(20):10109-10121. doi: 10.1128/jvi.76.20.10109-10121.2002.

5. Branche AR, Falsey AR. Parainfluenza virus infection. *Semin Respir Crit Care Med.* 2016;37(4):538-554. doi: 10.1055/s-0036-1584798.

6. R.E. Randall WCR. *The paramyxoviruses.* Boston, MA: Plenum Press; 1991.

7. Choppin PW. Multiplication of a myxovirus (sv5) with minimal cytopathic effects and without interference. *Virology.* 1964;23:224-233. doi: 10.1016/0042-6822(64)90286-7.

8. Fox CR, Parks GD. Parainfluenza virus infection sensitizes cancer cells to DNA-damaging agents: Implications for oncolytic virus therapy. *J Virol.* 2018;92(7). doi: 10.1128/jvi.01948-17.

9. Didcock L, Young DF, Goodbourn S, Randall RE. The v protein of simian virus 5 inhibits interferon signalling by targeting stat1 for proteasome-mediated degradation. *J Virol.* 1999;73(12):9928-9933. doi: 10.1128/jvi.73.12.9928-9933.1999.

10. Szegezdi E, Logue SE, Gorman AM, Samali A. Mediators of endoplasmic reticulum stress-induced apoptosis. *EMBO Rep.* 2006;7(9):880-885. doi: 10.1038/sj.embor.7400779.

11. Hetz C, Zhang K, Kaufman RJ. Mechanisms, regulation and functions of the unfolded protein response. *Nat Rev Mol Cell Biol.* 2020;21(8):421-438. doi: 10.1038/s41580-020-0250-z.

12. Prasad V, Greber UF. The endoplasmic reticulum unfolded protein response - homeostasis, cell death and evolution in virus infections. *FEMS Microbiol Rev.* 2021;45(5). doi: 10.1093/femsre/fuab016.

13. Varudkar N, Oyer JL, Copik A, Parks GD. Oncolytic parainfluenza virus combines with nk cells to mediate killing of infected and non-infected lung cancer cells within 3d spheroids: Role of type i and type iii interferon signaling. *J Immunother Cancer.* 2021;9(6). doi: 10.1136/jitc-2021-002373.

14. Ibrahim IM, Abdelmalek DH, Elfiky AA. Grp78: A cell's response to stress. *Life Sci.* 2019;226:156-163. doi: 10.1016/j.lfs.2019.04.022.

15. Yoshida H, Matsui T, Yamamoto A, Okada T, Mori K. Xbp1 mRNA is induced by ATF6 and spliced by IRE1 in response to er stress to produce a highly active transcription factor. *Cell.* 2001;107(7):881-891. doi: 10.1016/s0092-8674(01)00611-0.

16. Wu J, Chen S, Liu H, Zhang Z, Ni Z, Chen J, Yang Z, Nie Y, Fan D. Tunicamycin specifically aggravates ER stress and overcomes chemoresistance in multidrug-resistant

gastric cancer cells by inhibiting N-glycosylation. *J Exp Clin Cancer Res.* 2018;37(1):272. doi: 10.1186/s13046-018-0935-8.

17. Abdullahi A, Stanojcic M, Parousis A, Patsouris D, Jeschke MG. Modeling acute ER stress in vivo and in vitro. *Shock.* 2017;47(4):506-513. doi: 10.1097/shk.0000000000000759.

18. Jaskulska A, Janecka AE, Gach-Janczak K. Thapsigargin-from traditional medicine to anticancer drug. *Int J Mol Sci.* 2020;22(1). doi: 10.3390/ijms22010004.

19. Zhang S, Cao M, Fang F. The role of epigallocatechin-3-gallate in autophagy and endoplasmic reticulum stress (ERS)-induced apoptosis of human diseases. *Med Sci Monit.* 2020;26:e924558. doi: 10.12659/msm.924558.

20. Martinotti S, Ranzato E, Burlando B. (-)- epigallocatechin-3-gallate induces GRP78 accumulation in the er and shifts mesothelioma constitutive upr into proapoptotic er stress. *J Cell Physiol.* 2018;233(10):7082-7090. doi: 10.1002/jcp.26631.

21. D.T. Rutkowski VRL. Membrane targeting of proteins. In: G. Plopper DS, E. Sikorski, ed. *Lewin's cells*. 3 ed. Burlington, MA: Jones & Bartlett Learning 2015:301-354.

22. Satoh K, Matsu-Ura T, Enomoto M, Nakamura H, Michikawa T, Mikoshiba K. Highly cooperative dependence of sarco/endoplasmic reticulum calcium ATPase serca2a pump activity on cytosolic calcium in living cells. *J Biol Chem.* 2011;286(23):20591-20599. doi: 10.1074/jbc.M110.204685.

23. Lindner P, Christensen SB, Nissen P, Møller JV, Engedal N. Cell death induced by the ER stressor thapsigargin involves death receptor 5, a non-autophagic function of map1lc3b, and distinct contributions from unfolded protein response components. *Cell Commun Signal.* 2020;18(1):12. doi: 10.1186/s12964-019-0499-z.